processes

MDPI

Review

Bonding Processing and 3D Integration of High-Performance Silicon PIN Detector for ΔE-E telescope

Zhiyuan Zhu [1,*], Maoqiu Pu [1,2], Min Jiang [1], Sixiang Zhang [1] and Min Yu [3,*]

[1] College of Electronic and Information Engineering, Southwest University, Chongqing 400715, China
[2] Key Laboratory of Microelectronic Devices & Integrated Technology, Institute of Microelectronics, Chinese Academy of Sciences, Beijing 100029, China
[3] National Key Laboratory of Nano/Micro Fabrication Technology, School of Integrated Circuits, Peking University, Beijing 100871, China
* Correspondence: zyuanzhu@swu.edu.cn (Z.Z.); yum@pku.edu.cn (M.Y.)

Abstract: Currently, the integration method of silicon PIN radiation detectors faces challenges such as complex processes, poor reliability and thick dead layers. Novel integration methods based on metal bonding technology for realizing the integration of thick and thin PIN detectors are needed with the requirement of reducing signal crosstalk, package volume and weight. Combined with the current research on metal bonding technology, this paper presents an extensive review of metal bonding technology, especially metal Al bonding technology, to provide a certain reference to future research on the bonding processing of high-performance silicon PIN detector devices.

Keywords: high-performance silicon PIN detector; metal aluminum bonding; integrated silicon PIN detector; ΔE-E telescope

Citation: Zhu, Z.; Pu, M.; Jiang, M.; Zhang, S.; Yu, M. Bonding Processing and 3D Integration of High-Performance Silicon PIN Detector for ΔE-E telescope. *Processes* **2023**, *11*, 627. https://doi.org/10.3390/pr11020627

Academic Editor: Ioannis Spanopoulos

Received: 14 December 2022
Revised: 12 February 2023
Accepted: 15 February 2023
Published: 18 February 2023

Copyright: © 2023 by the authors. Licensee MDPI, Basel, Switzerland. This article is an open access article distributed under the terms and conditions of the Creative Commons Attribution (CC BY) license (https://creativecommons.org/licenses/by/4.0/).

1. Introduction

Since the appearance of semiconductor detectors in the early 1960s, semiconductors have been used to measure charged particles in space. After decades of dedicated effort, semiconductor detection technology has been greatly developed [1]. The silicon positive-intrinsic-negative (PIN) detector has become a hotspot in radiation detection research owing to its low reverse leakage current, strong adaptability to the environment and high stability [2–4]. The PIN detector is a structure that includes a layer of P-type semiconductor, a layer of N-type semiconductor, and the intrinsic semiconductor (I layer) between the two. The existence of the I layer can form a large depletion region, which increases the probability of particle injection, thus enhancing the energy resolution of the detector. Due to its thick barrier layer and large impedance coefficient, the PIN radiation detector can obtain a low dark current, high response and is easy to match with the focal plane array circuit. Further, this device structure can improve the quantum efficiency [5,6] and response speed by adjusting the eigen layer thickness.

Generally, the ΔE-E telescope for satellites are packaged based on printed circuit board (PCB) and two independent thin and thick Si-Pin detectors [7]. The ΔE-E telescope is widely used for heavy ion detection and tracking, high γ short-range particle detection and X-ray detection. When nuclear particles enter the ΔE-E telescope, they first interact with the thin detector and lose energy (ΔE), then interact with the thick detector and lose the residual energy (E-ΔE). Since ΔE is proportional to the particle mass and inversely proportional to E, the properties of particles can be obtained. To minimize the energy loss of ingoing high-energy particles in the ΔE-E detector, there is a certain requirement for the thickness of the thin detector (less than or equal to 100 μm). However, owing to the material characteristics of the Si material, the detector device is more likely to be damaged considering that the small thickness detector is subject to mechanical shock. Moreover, two independent detectors do not conform to the development trend of miniaturization and

integration. Particularly, the PCB board-based package requires heavy fixtures [4], which increase the system volume and weight. In addition, the two independent detectors will cause additional dead layers. Therefore, it is necessary to integrate one thin and one thick Si PIN radiation detector into one unit to provide mechanical support for the thin PIN detector, ensure mechanical reliability, reduce the dead layer and achieve high detection sensitivity.

Currently, there are many methods for establishing an integrated detector structure, such as forming a conductive buried layer by injecting high-energy particles [8–10] and using cobalt dioxide as a conductive buried layer [11]. However, most Si PIN radiation detectors use an Aluminum electrode for reducing the thickness of the dead zone. Nevertheless, dense oxide layers with stable chemical properties can easily grow on the Al surface, which typically requires the long-term application of high temperature and high pressure to achieve the bonding process, thus affecting the device reliability. Therefore, the optimization of bonding conditions is the key focus for integrated PIN detectors.

This paper discusses the bonding challenges of integrated Si PIN detectors. The existing metal bonding research, especially metal aluminum bonding research, has been analyzed. Research on the bonding challenges of the Si PIN detector has significant value for the three-dimensional integrated processing of microelectronic devices.

2. Silicon PIN Radiation Detector

The silicon PIN semiconductor detector is a novel particle injection detector, which consists of a P-type semiconductor layer, N-type semiconductor layer and an intrinsic semiconductor. Among them, the two layers on the side have heavy doping, while the middle layer has light doping. The advantages of the silicon PIN semiconductor are good spatial resolution, high sensitivity, and obvious output signal under the same irradiation dose. In actual use, multiple silicon PIN detectors are often combined [12].

For the thin PIN radiation detector, a 100 μm-thick silicon PIN detector is fabricated based on TMAH wet etching technology [13], as shown in Figure 1a. Further, in order to improve the reliability of the device, TMAH thinning technology based on an SOI silicon chip was proposed [14] for effective control of the thickness of the thin detector, as shown in Figure 1b. Figure 1c,d shows the structure of a typical 1.5 mm-thick silicon PIN radiation detector and the corresponding IV characteristic changes under ^{239}Pu-Be isotope neutron source radiation [15]. Furthermore, the guard ring was used to improve the performance of the thick detector. This kind of PIN diode with a bias guard ring can form a vertical current flowing outside the sensitive region in the case of forward bias, so as to avoid the change of forward IV characteristics caused by the reduction of excessive carrier lifetime. The silicon PIN radiation detector with a thickness of 1.5 mm and a width of 1 mm and containing the guard ring structure was prepared as a fast neutron detector [16]. The test results show that diodes with a forward-biased guard ring achieve 7% higher sensitivity under 1 mA constant current source. The percentage rises to 15% when 5 mA or 10 mA constant current source is applied, as shown in Figure 1e,f. In addition, a ring-type silicon PIN radiation detector structure (1.5 mm thick) was proposed with radiation detection sensitivity adjusted by the P^+ and N^+ distance [17], as shown in Figure 1g,h.

ΔE-E telescope Structure

Currently, the silicon PIN semiconductor radiation detector is mainly used for the ΔE-E telescope to identify charged particles (electrons, protons, α particles, heavy ions), nuclear reactions and primitive cosmic ray particles.

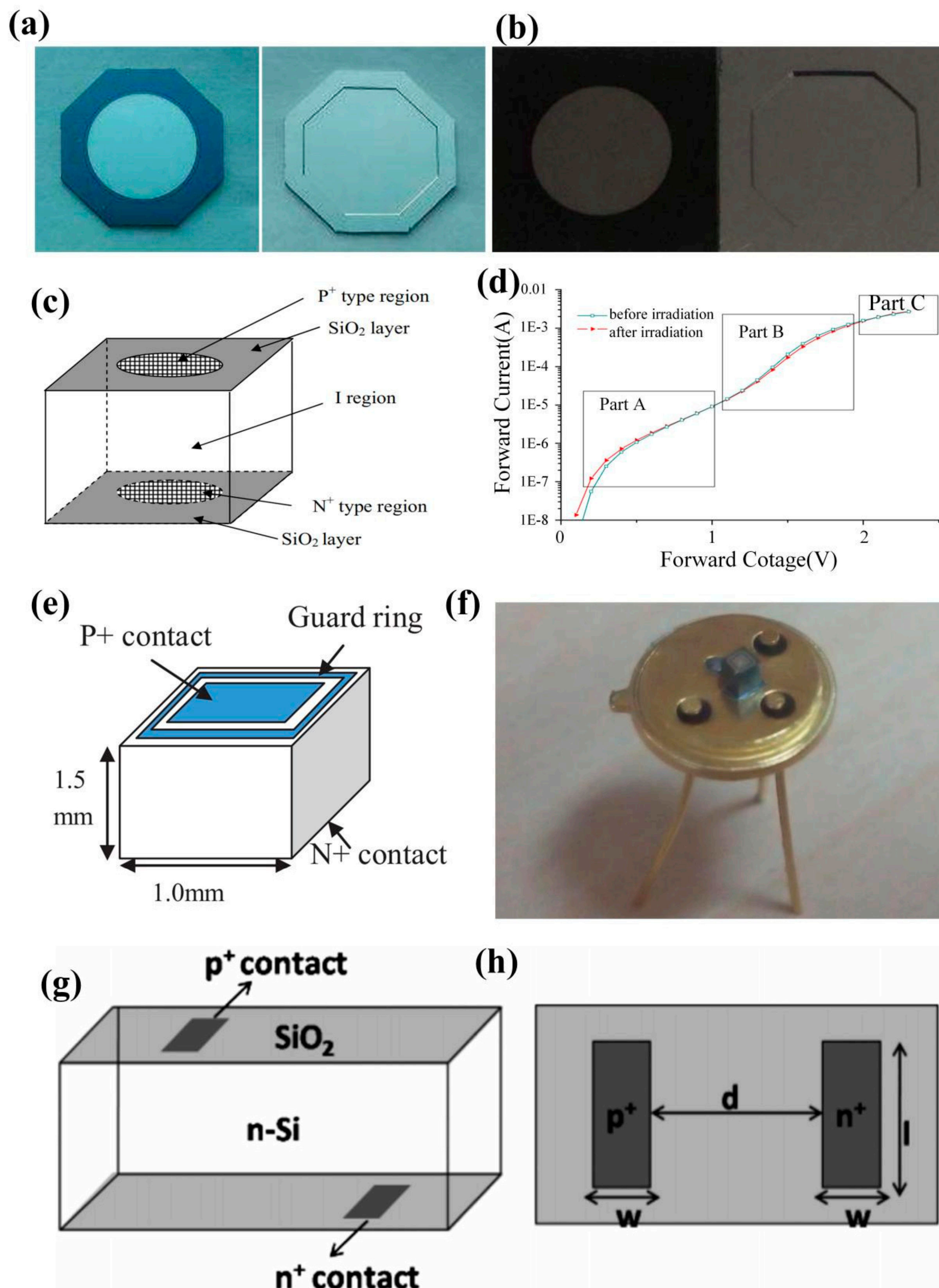

Figure 1. (**a**,**b**) Picture of thin PIN detector [13,14]; (**c**) structural diagram of 1.5 mm-thick silicon PIN radiation detector [15]; (**d**) IV characteristic change of 1.5 mm-thick silicon PIN radiation detector [15]; (**e**) structural diagram of 1.5 mm-thick silicon PIN detector based on guard ring [16]; (**f**) photos after the detector is packaged [16] (**g**,**h**) bilateral PIN diode structure [17].

Most ΔE-E telescopes are constructed using a thin silicon PIN detector and a thick silicon PIN detector through PCB packaging [4]. The individual detectors are typically packaged with PCB boards. However, this packaging method typically requires bulky fixed devices (Figure 2). Additionally, two individual detectors result in more dead layers. Therefore, an attractive construction method is to integrate the thin PIN radiation detector and the thick PIN radiation detector to form an integral unit to solve the problem of mechanical reliability. This integrated structure is also conducive to reducing the thickness of the dead layer and improving the detection sensitivity.

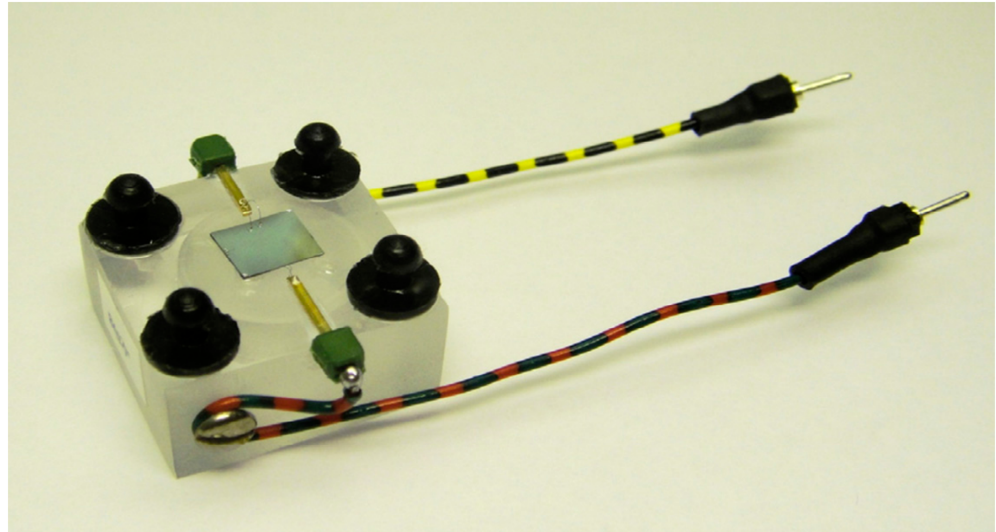

Figure 2. Fixtures required for the construction of ΔE-E telescope with separated silicon PIN radiation detector [4].

To manufacture this integrated detector structure, one method is to use a high-energy particle injection to form a conductive buried layer as the common electrode of the thick PIN detector and thin PIN detector [8–10], then conduct low-energy particle injection doping to form another electrode of the thick and thin PIN detectors, wherein the conductive buried layer uses another injection doping extraction electrode. The second method is to make thick PIN detectors by diffusion doping, then make thin PIN detectors by epitaxy, [18,19] (the process flow is shown in Figure 3a [18]). Another method is to use cobalt silicide as a conductive buried layer to form a ΔE-E nuclear radiation detector. The process flow is shown in Figure 3b [11]. However, these methods have many problems, such as the complex process, great difficulty and inability to ensure the process success rate. A novel integration method is to use bonding technology to realize the integration of thick and thin PIN detectors. This method can effectively reduce the package volume and weight, but there are certain requirements for achieving the bonding conditions. For example, high temperature and high pressure are likely to cause the failure of silicon PIN radiation detectors, and a longer bonding time is not conducive to the improvement of production efficiency.

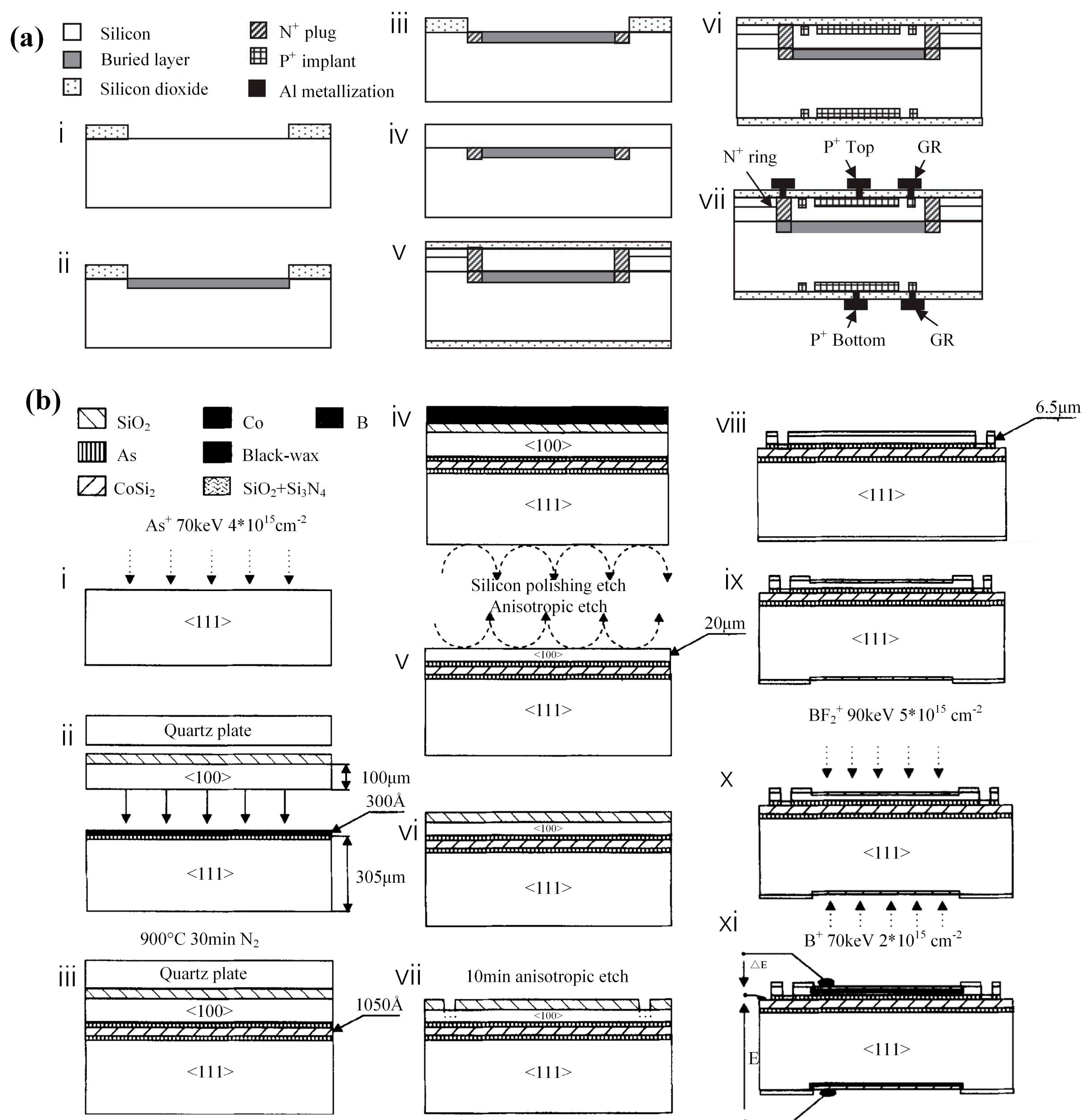

Figure 3. Process flow diagram of integrated silicon PIN radiation detector based on (**a**) epitaxial growth [18] and (**b**) cobalt silicide as the conductive buried layer [11].

3. From Metal Bonding to Metal Aluminum Bonding

Metal bonding technology is a common material connection method nowadays. This technology refers to the face-to-face bonding of two wafers through a pure metal or alloy, which relies on metal bonding, diffusion between a metal and the wafer surface, metal melting and so on [20]. Metal bonding includes eutectic and diffusion methods, metal eutectic bonding uses alloy materials to be formed by two or more metals in a certain proportion to realize the transformation from the solid phase to the liquid phase at a low temperature. The eutectic metal alloys melt during the bonding process and automatically realize the flatness of the interface; therefore, the requirements for the morphology of the wafer bonding surface are not strict [21]. The commonly used diffusion-bonded metal materials are Au, Cu, and Al, which have excellent ductility and high diffusivity. Diffusion bonding is typically completed at 350–500 °C, and due to the process, temperature is relatively high; relatively high pressure is required to achieve close contact between the bonded

metal surfaces. Bonded metals provide mechanical adhesion and electrical interconnection. Metal bonding technology is characterized by a simple process, the bonding area is far away from the active area of the device and improves the thermoelectric performance of the device.

The main process steps of metal bonding technology are similar to those of the adhesive bonding method. First, the surface of the bonding material must be cleaned and mirror-polished to make the surface flat, clean and free of impurities. Then, the metal film is vapor-deposited onto the material by electroplating, electron beam evaporation and so on. After corrosion and recleaning, the two wafers are overlaid face to face, and certain pressure is applied through the bonding device to realize the bonding between the wafers. For different wafer materials, the bonding process can be carried out under room temperature or high temperature annealing conditions. Finally, chemical solutions are used to etch the metal-bonded wafers and remove the substrate for the subsequent processing of the devices. Due to the excellent conductivity of the metal bonding layer, metal bonding is often used for 3D integrated interconnection. Compared with the main process steps of metal bonding, the process of metal bonding increases the treatment of the Si through-hole.

For different metals, particularly aluminum-based ones, bonding technology has attracted considerable attention. Because aluminum has high electrical conductivity and thermal conductivity, as well as good adhesion to silicon and silicon dioxide, it has been used as the standard metallization in the silicon-integrated circuit industry. Additionally, Al is typically used as the electrode material of the Si PIN radiation detector. The Al–P^+ contact minimizes the thickness of the dead layer of the detector [22]. However, a problem that cannot be ignored is the fact that Al metal bonding generates various intermetallic compounds after being kept at a high temperature for a long time. For example, five thermodynamic stable intermetallic compounds ($AuAl_2$, AuAl, Au_2Al, Au_5Al_2, and Au_4Al) can be generated in the hetero metallic bonding process of Al. Among them, Au_2Al exhibits brittleness and high resistance, which is one of the main factors affecting the bonding effect [23]. In the process of Cu–Al bonding, interface atoms can easily form intermetallic compounds ($CuAl_2$, CuAl, Cu_4Al_3, Cu_3Al_2, and Cu_9Al_4) through diffusion [24]. The crystal structures of these intermetallics are different to those of bonded wafer metals. Owing to the mismatch of the lattice constant and the large difference in the thermal expansion coefficient between the metal compounds, large internal stresses are generated during the growth of intermetallic compounds, which reduces the bonding strength of the interface. Moreover, these intermetallics have high hardness and high resistivity, which increases the brittleness and reduces the conductivity of the bonding system after nucleation and growth. Additionally, for good wafer bonding, the bonding toughness and contact area per unit area should be as high as possible. However, the actual surface has micro roughness; therefore, the actual contact area between the contact surfaces is typically much smaller than the nominal contact area [25], which further influences the bonding effect. Therefore, the bonding between metals generally requires extremely high processing temperature and pressure [26,27]. Thus, in addition to improving the bond strength, this study also focuses on further optimizing the bonding conditions after reaching a certain bond strength.

At present, Tong [28] reported a method of room-temperature metal direct bonding in air between aligned metal posts on oxide-covered silicon wafers without externally applied pressure or force. That is, a thin layer of gold is deposited on the metal column to achieve room temperature bonding of metal columns other than gold. Different from this method, some researchers have added ion sputtering technology on the basis of process optimization. For example, Kurashima et al. [29] used the hot embossing process to press the surface grinding tool onto the metal film on the wafer at a high temperature. After the metal surface had been flattened, the Ar beam was used to activate the metal surface to achieve bonding at room temperature. Higurashi et al. [30] carried out bonding by contact under ambient air, and applied static pressure after cleaning the surface of the Au film with Ar radio frequency plasma. At the bonding temperature of 100 °C, the die-shear strength exceeded the failure criteria of MIL-STD-883. Based on the process optimization, these

provide a certain technical reference for Al–Al metal low-temperature bonding. In the series of studies on Al-based metal bonding schemes, the American Analog Devices Company applied a pressure of 30 MPa at the bonding temperature of 445 °C to achieve Al ring bonding with a width of 4–90 μm [31]. Further, they achieved Al ring bonding with a width of 3–150 μm on the wafer [32]. Dragoi et al. [33] of EV Group Australia investigated the effects of the bonding temperature, bonding time and bonding atmosphere on the quality of Al–Al bonding. Malik et al. [34] compared the dicing yield of Al–Al bonding and the cohesive Si fracture results obtained under different bonding temperatures and pressures, and found that strong Al–Al hot-pressed bonds can be obtained at 450 °C or above. Further, Malik et al. [27,35] performed Al–Al direct bonding at the bonding temperatures of 400, 450 and 550 °C, respectively, under different bonding forces. Their results revealed that, under experimental bonding conditions, the bonding strength increased with the bonding temperature and bonding force. Figure 4 shows the failure surface photos of typical Al–Al-bonded samples prepared under different bonding temperatures (400–550 °C) and bonding pressures (18–36 kN; converted bonding pressures: 34–69 MPa). Generally, Al–Al bonding requires high temperature, high pressure and long bonding time. However, high temperature and high pressure may cause the failure of the silicon PIN radiation detector, and longer bonding time is not conducive to the improvement of production efficiency. Therefore, the influence of primary oxides, surface roughness and other materials should be further investigated with regard to achieving successful bonding at a lower temperature.

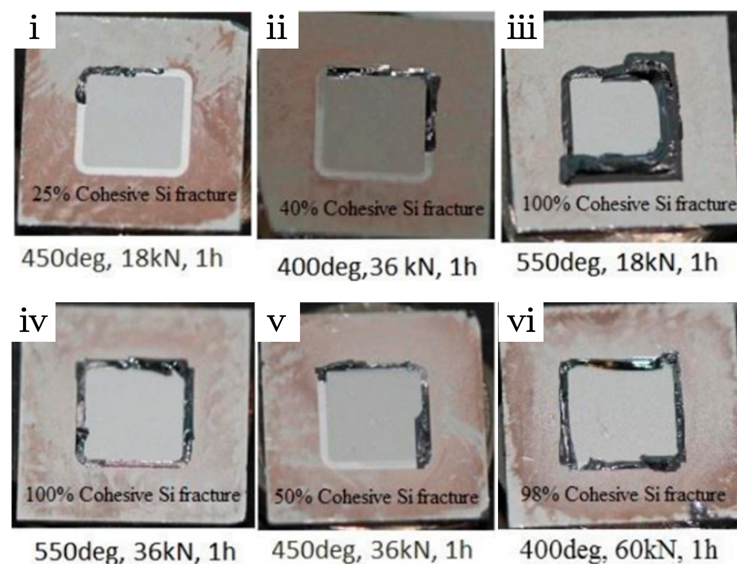

Figure 4. Effect of bonding temperature and pressure influence on Al–Al bonding quality [35].

3.1. Native Oxide

The native oxide layer, with highly stable chemical properties on the aluminum surface, cannot be removed by conventional methods [36]. The stable oxide layer acts as a barrier and it inhibits the diffusion of Al atoms on the bonding interface [37]. Generally, effective Al–Al wafer bonding requires a processing temperature above 300 °C and higher contact pressure. To avoid the influence of primary oxide produced by Al in the bonding process, a feasible solution is to adopt a dry surface pretreatment process for the removal of primary oxides. For example, Hinterreiter et al. [38] used Ar plasma treatment to remove surface oxides while processing the wafer under an ultra-high vacuum, and achieved the Al–Al bonding of amorphous wafer pairs at 150 °C. Atomic force microscopy (AFM) images of the Al wafer surfaces for standard deposition and the aluminum low pressure seed (ALPS) wafers are shown in Figure 5a,b. Schulze et al. [37] modified the etching mask during the wafer manufacturing process to improve the quality of the aluminum bonding pad surface and achieve improved bonding. At temperatures as low as 250 °C, they achieved a

high bonding yield of >85% and contact resistance in the mΩ range. Based on the results obtained by several groups of wafer bonding experiments, Rebhan et al. [36] found that a wafer with a blank Al film can reduce the bonding temperature to 150 °C, while a wafer with a frame Al pattern can reduce the bonding temperature to 100 °C.

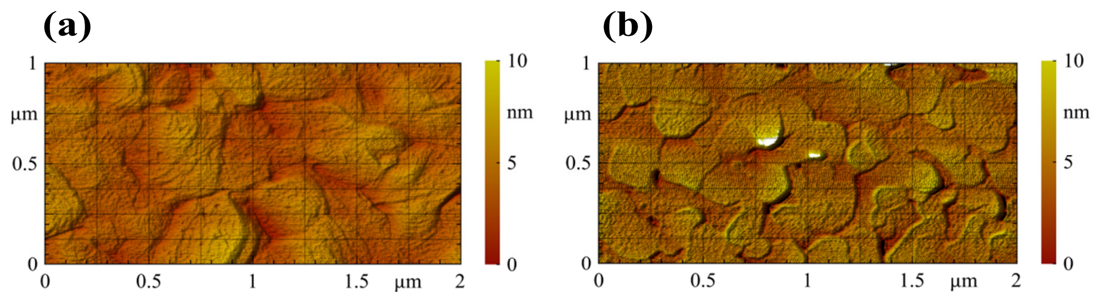

Figure 5. AFM images [38] of (**a**) the Al wafer surfaces for standard deposition, (**b**) the Al wafer surfaces for the ALPS wafers.

3.2. Surface Roughness

The surface roughness of bonded wafers is a key parameter affecting the Al–Al bonding quality [39–41]. After Al–Al bonding, it is expected that a higher bonding strength can be obtained when the surface roughness is less than or equal to 1 nm. However, when using standard Al deposition technology, the surface roughness value is much higher than this requirement (typically 5–8 nm). Typically, a stylus profilometer is used to measure the surface flatness and yield strength of the wafer to be bonded, and an atomic force microscope is used to measure the microroughness of the wafer surface. For materials that exhibit work hardening, Leong et al. [42] associated the surface roughness and applied load with the actual contact area. Thereby, a surface roughness acquisition model was established to provide a quantitative estimate of the actual contact area achieved in thermocompression bonding as a function of the surface topographic characteristics, so as to describe the surface roughness according to the average radius of curvature, peak height, and density of surface roughness. From the viewpoint of reducing the surface roughness, Schulze et al. [43] reduced the surface roughness of sputtered aluminum bonding pads below 2 nm by optimizing the aluminum deposition parameters. On this basis, a wafer level Al–Al thermocompression bonding process at a temperature between 300–500 °C with very low contact resistance was developed. This process has extremely low contact resistance, accurate alignment, and high uniformity. According to the result, the temperature of 300 °C is sufficient for achieving strong Al–Al wafer bonding.

3.3. Optimization of Intermediate Layer Materials

Considering the influence of different materials on the Al–Al bonding process, many studies have developed alternative methods to achieve low temperature bonding from intermediate layer materials, so as to reduce the influence of primary oxides and chip surface roughness as much as possible. For example, the bonding performance of Al deposited on Si is different to that of Al deposited on SiO_2. The Al grains deposited on SiO_2 are more mixed, and the required bonding pressure and temperature for the fracture are lower [44]. Therefore, when a SiO_2 layer appears in Al, the bonding temperature, pressure, and time can be reduced to a certain extent without reducing the bonding strength [27]. Zhu et al. [45] realized the bonding of an Al-coated silicon wafer with vertical electronic interconnection using PPC and a graphite particle interlayer under the low bonding pressure of 0.1 MPa and low temperature of 150 °C. To date, various studies have used ionomers for auxiliary bonding. Lin et al. [46] proposed a method of direct metal contact interconnection by using plasma-assisted low-temperature oxidation bonding to provide the necessary mechanical bonding strength. They established an electrical connection in the bonding annealing step and achieved the integration of MEMS and CMOS, but the annealing temperature

was higher (435 °C). Chang et al. [47] introduced a method of removing the primary aluminum oxide using argon plasma and tin (Sn) as the bonding interlayer on the basis of the electroplating aluminum bonding ring.

However, applying a thin layer of Sn on the Al surface as an oxidation barrier layer and bonding interlayer can promote Al–Al bonding to a certain extent. The Al–Al wafer bonding method with an intermediate tin layer has the advantages of low bonding temperature, low bonding pressure and short bonding time compared with Al–Al direct bonding [48]. For example, Satoh et al. [49] achieved long-term stable Al–Al bonding at 400 °C by applying an anti-oxidation Sn layer on the aluminum surface. Zhu et al. [48] considered the relationship between the bonding strength of Al–Al wafers containing intermediate tin layers and the bonding temperature and time, and found that a higher bonding strength can be obtained at an appropriate low bonding temperature and appropriate short bonding time according to the scanning electron microscope morphology of the corresponding shear strength of the fracture surface under different bonding conditions. When the bonding temperature was 280 °C and the bonding time was 1 min, the average shear strength reached 11 MPa. Additionally, the authors achieved the bonding of a silicon wafer coated with an aluminum film and thin tin film as the intermediate layer under the following conditions: bonding pressure of 0.25 MPa, bonding time of 3 min, bonding temperature of 280 °C, and average bonding strength of 9.9 MPa [50]. By using a scanning microscope to observe the cross-section and port morphology of the composite, they found that applying pressure before heating has a certain positive significance for obtaining a uniform adhesive layer.

4. Fabrication of the Integrated Detector

In order to minimize the thickness of the dead layer, silicon PIN detectors generally use metal Al electrodes. Due to the surface oxide layer of the metal Al electrode, Al–Al direct bonding usually requires certain bonding conditions. However, extreme bonding conditions will have a great adverse impact on the reliability of devices, especially on the performance of thin detectors. To overcome the above problems, our group introduced Al–Sn–Al bonding technology into the integration of thick and thin PIN detectors [7]. The whole integration process is carried out in a low temperature and pressure environment, which has the advantages of flexibility, reliability, good repeatability and the ability to bond PIN detectors with different thickness and different sensitive areas.

The typical fabrication processes include: First, thick PIN detectors and thin detectors were fabricated with Al electrodes. Then, the PIN detector is attached to the silicon wafer by a photoresist, and the photoresist is cured by heating. After that, the detectors are placed in the PVD cavity for in situ Ar plasma sputtering cleaning to remove native aluminum oxide. Then, put the Sn layer in the same vacuum chamber and sputter it onto the aluminum layer in situ. After the Sn layer was deposited, the samples were placed in lactone to dissolve the photoresist. After drying with nitrogen, a PIN detector with an Sn layer was obtained. After that, the thin and thick silicon PIN detectors were stacked. The devices were pressed together at a force of 7.5 N in a vacuum chamber at 9×10^{-4} mbar and heated to 330 °C, followed by immediate cooling to avoid the obvious impact of the bonding process on PIN device quality. The detectors were successfully bonded and taken out from a wafer bonder at 200 °C. Figure 6 shows the fabrication steps of an integrated PIN detector structure based on Al–Sn–Al bonding. After testing, there is no significant difference in the electronic performance of thin and thick silicon PIN detectors before and after bonding, and the Al–Sn–Al bonding integration technology has sufficient mechanical strength. The reverse I-V characteristics of typical silicon PIN detectors are shown in Figure 7a,b. Figure 7c,d shows the reverse I–V curve of typical bonded 300 μm and 100 μm-thick PIN detector structures. The success of this bonding method provides a certain reference value for subsequent detector integration by optimizing the interlayer materials, reducing the surface roughness and removing the surface oxides.

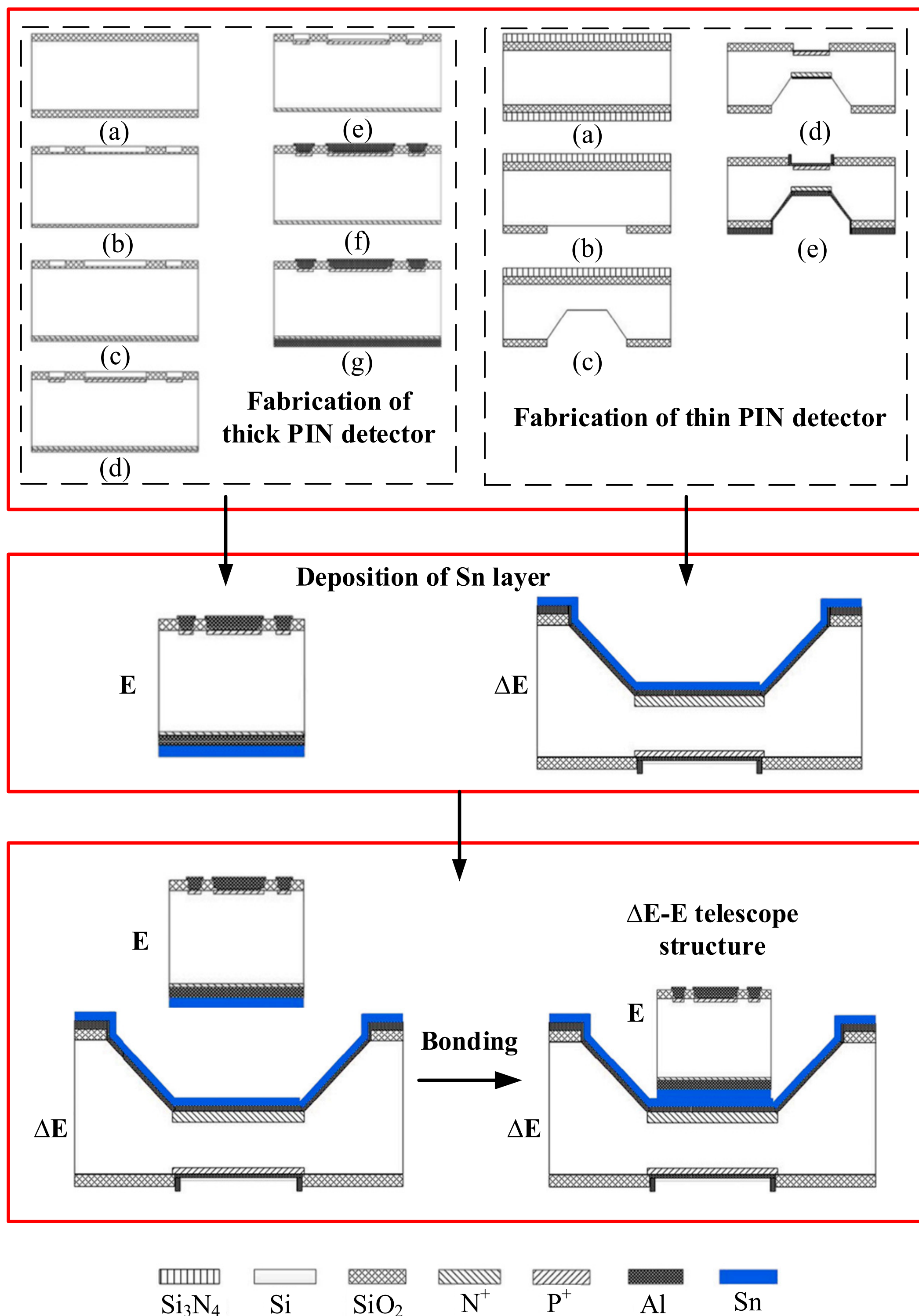

Figure 6. Fabrication steps of integrated PIN detector structure based on Al–Sn–Al bonding [7].

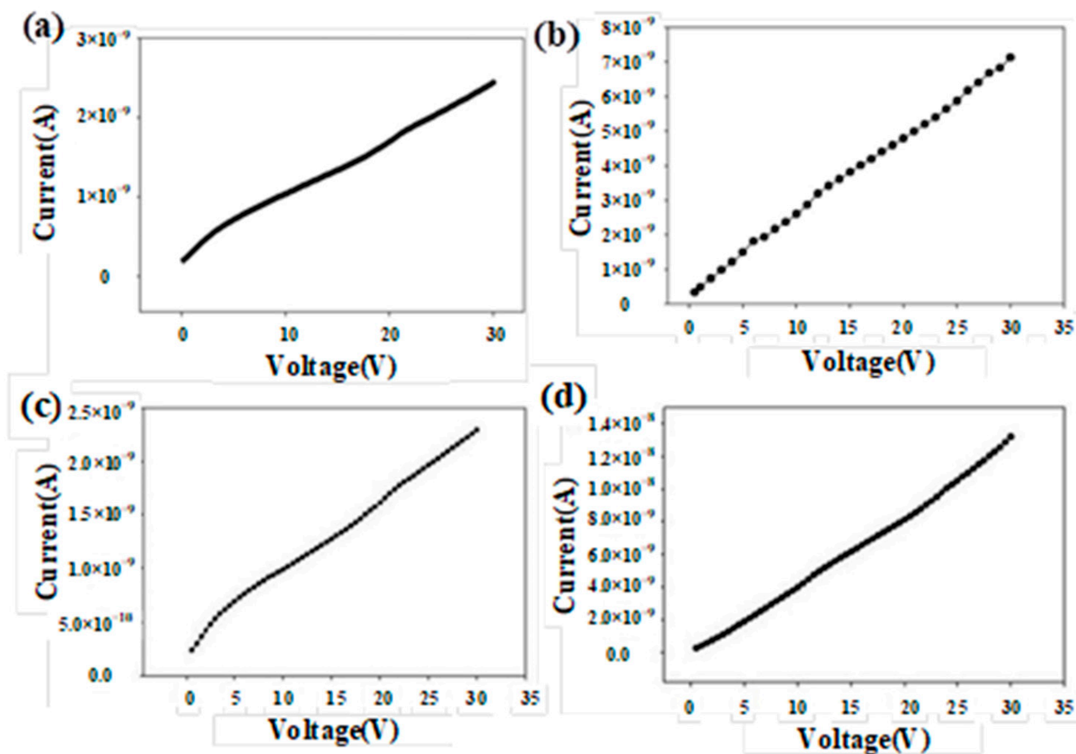

Figure 7. Reverse IV curves of (**a**) 300 µm-thick (**b**) 100 µm-thick PIN detector (**c**) typical bonded 300 µm and (**d**) 100 µm-thick PIN detector structure [7].

5. Conclusions

This paper analyzes the bonding challenges of a silicon PIN detector, especially the metal bonding problem. Traditional metal wafer bonding requires an extremely high processing temperature and pressure, mainly owing to the natural chemically stable metal oxide layer, which hinders the diffusion of metal atoms between the two metal layers. Additionally, the surface roughness, bonding temperature and bonding pressure of bonded wafers have certain effects on the final bonding strength. Based on existing work, achieving good bonding strength at low bonding temperature and pressure is important for the future of 3D-integrated processing and the performance optimization of Si PIN detectors.

Author Contributions: Writing—Review and project administration, Z.Z.; writing—original draft preparation and editing, M.P.; investigation, M.J.; formal analysis, S.Z.; supervision, M.Y. All authors have read and agreed to the published version of the manuscript.

Funding: This paper is supported by the Opening Project of Key Laboratory of Microelectronic Devices & Integrated Technology, Institute of Microelectronics, Chinese Academy of Sciences, and National Natural Science Foundation of China (62074132).

Data Availability Statement: No new data were created or analyzed in this study. Data sharing is not applicable to this article.

Conflicts of Interest: The research was conducted in the absence of any commercial or financial relationships that could be construed as a potential conflict of interest.

References

1. Shi, W.; Chen, H.; Zou, H.; Zou, J.; Tian, D.; Ning, B.; Zhang, L. The PIN detector parallel application. *Nucl. Electron. Detect. Technol.* **2007**, *27*, 908–910.
2. Yu, B.; Zhao, K.; Yang, T.; Jiang, Y.; Fan, X.; Lu, M.; Han, J. Process effects on leakage current of Si-PIN neutron detectors with porous microstructure. *Phys. Status Solidi (A)* **2017**, *214*, 1600900. [CrossRef]
3. Li, H.X.; Li, Z.K.; Wang, F.C.; Li, R.-H.; Chen, C.H.; Wang, X.H.; Rong, X.J.; Liu, F.Q.; Wang, Z.S.; Li, C.Y.; et al. Application of stratified implantation for silicon micro-strip detectors. *Chin. Phys. C* **2015**, *39*, 066005. [CrossRef]

4. Abdel, N.S.; Pallon, J.; Ros, L.; Borysiuk, M.; Elfman, M.; Kristiansson, P.; Nilsson, E.C. Characterizations of new ΔE detectors for single-ion hit facility. *Nucl. Instrum. Methods Phys. Res. Sect. B Beam Interact. Mater. At.* **2014**, *318*, 281–286. [CrossRef]
5. McClintock, R.; Yasan, A.; Mayes, K.; Shiell, D.; Darvish, S.R.; Kung, P.; Razeghi, M. High quantum efficiency AlGaN solar-blind pin photodiodes. *Appl. Phys. Lett.* **2004**, *84*, 1248–1250. [CrossRef]
6. Wang, H.; Liu, J.; Niu, N.; Shen, G.; Zhang, S. Enhanced performance of p-GaN by Mg δ doping. *J. Cryst. Growth* **2007**, *304*, 7–10. [CrossRef]
7. Zhu, Z.; Yu, M.; Jin, Y. Fabrication of integrated silicon PIN detector based on Al-Sn-Al bonding for ΔE-E telescope application. *Microelectron. Eng.* **2021**, *247*, 111599. [CrossRef]
8. Tran, L.T.; Bolst, D.; Guatelli, S.; Biasi, G.; Fazzi, A.; Sagia, E.; Prokopovich, D.A.; Reinhard, M.I.; Keat, Y.C.; Petasecca, M.; et al. High spatial resolution microdosimetry with monolithic ΔE-E detector on 12C beam: Monte Carlo simulations and experiment. *Nucl. Instrum. Methods Phys. Res. Sect. A Accel. Spectrometers Detect. Assoc. Equip.* **2018**, *887*, 70–80. [CrossRef]
9. Tudisco, S.; Amorini, F.; Cabibbo, M.; Cardella, G.; De Geronimo, G.; Di Pietro, A.; Fallica, G.; Figuera, P.; Musumarra, A.; Papa, M.; et al. A new large area monolithic silicon telescope. *Nucl. Instrum. Methods Phys. Res. Sect. A Accel. Spectrometers Detect. Assoc. Equip.* **1999**, *426*, 436–445. [CrossRef]
10. Kostka, A.; Kalbitzer, S. Ion Implanted Buried Layers Applied for Nuclear Detector Telescopes. In *Ion Implantation in Semiconductors*; Springer: Boston, MA, USA, 1975; pp. 689–694.
11. Thungström, G.; van Veldhuizen, E.J.; Westerberg, L.; Norlin, L.-O.; Petersson, C. Fabrication of an integrated ΔE-E-silicon detector by wafer bonding using cobalt disilicide. *Nucl. Instrum. Methods Phys. Res. Sect. A Accel. Spectrometers Detect. Assoc. Equip.* **1997**, *391*, 315–328. [CrossRef]
12. Evensen, L.; Westgaard, T. *Thin Detectors for the CHICSi {Delta} EE Telescope*; IEEE Service Center: Piscataway, NJ, USA, 1996.
13. Wang, S.; Yu, M.; Tian, D.; Liu, H.; Wang, P.; Shi, B.; Hu, A.; Du, H.; Wang, J.; Jin, Y. Fabrication and characterization of thin silicon PIN detectors. *ECS Trans.* **2014**, *60*, 1165. [CrossRef]
14. Dong, X.; Yu, M.; Tian, D.; Wang, J.; Xiang, H.; Jin, Y. Fabrication of thin silicon PIN detector based on wafer bonding technology. *ECS Trans.* **2012**, *44*, 1413. [CrossRef]
15. Fan, C.; Yu, M.; Yang, F.; Tian, D.; Wang, J.; Jin, Y. Research on Silicon PIN Neutron Dose Detector. *ECS Trans.* **2012**, *44*, 1401. [CrossRef]
16. Zhang, Z.; Yu, M.; Zhu, Z.; Wang, H.; Huang, Y.; Jin, Y. Fabrication of 1.5 mm thickness silicon pin fast neutron detector with guard ring structure. In *Proceedings of the 2016 China Semiconductor Technology International Conference (CSTIC), Shanghai, China, 13–14 March 2016*; IEEE: Piscataway, NJ, USA, 2016; pp. 1–3.
17. Hu, A.Q.; Yu, M.; Zhou, C.Z.; Fan, C.; Liu, C.C.; Wang, S.N.; Shi, B.H.; Qi, L.; Wang, J.Y.; Jin, Y.F. Bilateral PIN diode for fast neutron dose measurement. *IEEE Trans. Nucl. Sci.* **2014**, *61*, 1311–1315. [CrossRef]
18. Topkar, A.; Singh, A.; Santra, S.; Mukhopadhyay, P.; Chatterjee, A.; Choudhury, R.; Pithawa, C. Development of integrated ΔE–E silicon detector telescope using silicon planar technology. *Nucl. Instrum. Methods Phys. Res. Sect. A Accel. Spectrometers Detect. Assoc. Equip.* **2011**, *654*, 330–335. [CrossRef]
19. Kordyasz, A.J.; Kulczycka, E. Double sided strip monolithic silicon E–ΔE telescope produced by Quasi-Selective Epitaxy. *Nucl. Instrum. Methods Phys. Res. Sect. A Accel. Spectrometers Detect. Assoc. Equip.* **2008**, *596*, 131–133. [CrossRef]
20. Xie, Z.; Wu, H.; Lao, Y.; Liu, C.; Cao, M. Metallic bonding technique and applications to optoelectronic devices. *Laser & Optoelectronics Progress.* **2007**, *44*, 31–37.
21. Xu, C.; Xu, Y.; Yang, Y.; Yang, Z. Application of the Au/Sn Eutectic Bonding Technology in the Packaging of MEMS. *Micronanoelectronic Technology.* **2014**, *51*, 131–135. [CrossRef]
22. Jaklevic, J.M.; Walton, J.T.; McMurray Jr, R.E.; Madden, N.W.; Goulding, F.S. Semiconductor detector performance for low-energy x-rays. *Nucl. Instrum. Methods Phys. Res. Sect. A Accel. Spectrometers Detect. Assoc. Equip.* **1988**, *266*, 598–601. [CrossRef]
23. Cheng, C.; Xu, Y.; Liu, H. Reliability Analysis of Au-Al Bimetallic Bonding. *Semicond. Technol.* **2011**, *36*, 562–565.
24. Yue, A.; Peng, K.; Zhou, L.; Zhu, J.; Li, D. The formation rule and controlling method of intermetallic compounds in Al/Cu bonding system. *Materials Reports.* **2013**, *27*, 117–120.
25. Greenwood, J.S.; Williamson, J.B.P. Contact of nominally flat surfaces. *Proc. R. Soc. London. Ser. A. Math. Phys. Sci.* **1966**, *295*, 300–319.
26. Froemel, J.; Baum, M.; Wiemer, M.; Roscher, F.; Haubold, M.; Jia, C.; Gessner, T. Investigations of thermocompression bonding with thin metal layers. In *Proceedings of the 2011 16th International Solid-State Sensors, Actuators and Microsystems Conference, Beijing, China, 5–9 June 2011*; IEEE: Piscataway, NJ, USA, 2011; pp. 990–993.
27. Malik, N.; Schjølberg-Henriksen, K.; Poppe, E.U.; Taklo, M.M.V.; Finstad, T. Impact of SiO_2 on Al–Al thermocompression wafer bonding. *J. Micromechanics Microengineering* **2015**, *25*, 035025. [CrossRef]
28. Tong, Q.Y. Room temperature metal direct bonding. *Appl. Phys. Lett.* **2006**, *89*, 182101. [CrossRef]
29. Kurashima, Y.; Maeda, A.; Takigawa, R.; Takagi, H. Room temperature wafer bonding of metal films using flattening by thermal imprint process. *Microelectron. Eng.* **2013**, *112*, 52–56. [CrossRef]
30. Higurashi, E.; Imamura, T.; Suga, T.; Sawada, R. Low-temperature bonding of laser diode chips on silicon substrates using plasma activation of Au films. *IEEE Photonics Technol. Lett.* **2007**, *19*, 1994–1996. [CrossRef]
31. Martin, J. Wafer capping of MEMS with fab-friendly metals. *Reliab. Packag. Test. Charact. MEMS/MOEMS VI* **2007**, *6463*, 204–209.

32. Yun, C.H.; Martin, J.R.; Tarvin, E.B.; Winbigler, J.T. Al to Al wafer bonding for MEMS encapsulation and 3-D interconnect. In *Proceedings of the 2008 IEEE 21st International Conference on Micro Electro Mechanical Systems, Tucson, AZ, USA, 13–17 January 2008*; IEEE: Piscataway, NJ, USA, 2008; pp. 810–813.
33. Dragoi, V.; Mittendorfer, G.; Burggraf, J.; Wimplinger, M. Metal thermocompression wafer bonding for 3D integration and MEMS applications. *ECS Trans.* **2010**, *33*, 27. [CrossRef]
34. Malik, N.; Schjølberg-Henriksen, K.; Poppe, E.; Finstad, T.G. Al-Al thermocompression bonding for wafer-level MEMS packaging. In *Proceedings of the 2013 Transducers & Eurosensors XXVII: The 17th international Conference on Solid-State Sensors, Actuators and Microsystems (TRANSDUCERS & EUROSENSORS XXVII), Barcelona, Spain, 16–20 June 2013*; IEEE: Piscataway, NJ, USA, 2013; pp. 1067–1070.
35. Malik, N.; Schjølberg-Henriksen, K.; Poppe, E.; Taklo, M.; Finstad, T. AlAl thermocompression bonding for wafer-level MEMS sealing. *Sens. Actuators A Phys.* **2014**, *211*, 115–120. [CrossRef]
36. Rebhan, B.; Hinterreiter, A.; Malik, N.; Schjølberg-Henriksen, K.; Dragoi, V.; Hingerl, K. Low-temperature aluminum-aluminum wafer bonding. *ECS Trans.* **2016**, *75*, 15. [CrossRef]
37. Schulze, S.; Vob, T.; Kruger, P.; Fraschke, M.; Kulse, P.; Wietstruck, M. Influence of Process Parameters on Surface Activated Aluminum-to-Aluminum Wafer Bonding. *IEEE Trans. Compon. Packag. Manuf. Technol.* **2022**, *12*, 578–586. [CrossRef]
38. Hinterreiter, A.P.; Rebhan, B.; Flötgen, C.; Dragoi, V.; Hingerl, K. Surface pretreated low-temperature aluminum–aluminum wafer bonding. *Microsyst. Technol.* **2018**, *24*, 773–777. [CrossRef]
39. Rebhan, B.; Wimplinger, M.; Hingerl, K. Impact factors on low temperature Cu-Cu wafer bonding. *ECS Trans.* **2014**, *64*, 369. [CrossRef]
40. Panigrahi, A.K.; Bonam, S.; Ghosh, T.; Vanjari SR, K.; Singh, S.G. Low temperature, low pressure CMOS compatible Cu-Cu thermo-compression bonding with Ti passivation for 3D IC integration. In *2015 IEEE 65th Electronic Components and Technology Conference (ECTC)*; IEEE: Piscataway, NJ, USA, 2015; pp. 2205–2210.
41. Rebhan, B.; Hingerl, K. Physical mechanisms of copper-copper wafer bonding. *J. Appl. Phys.* **2015**, *118*, 135301. [CrossRef]
42. Leong, H.L.; Gan, C.L.; Thompson, C.V.; Pey, K.L.; Li, H.Y. Application of contact theory to metal-metal bonding of silicon wafers. *J. Appl. Phys.* **2007**, *102*, 103510. [CrossRef]
43. Schulze, S.; Wietstruck, M.; Fraschke, M.; Kerepesi, P.; Kurz, H.; Rebhan, B.; Kaynak, M. Optimization of a BEOL aluminum deposition process enabling wafer level al-al thermo-compression bonding. In *2019 IEEE 69th Electronic Components and Technology Conference (ECTC)*; IEEE: Piscataway, NJ, USA, 2019; pp. 218–224.
44. Taklo, M.V.; Schjolberg-Henriksen, K.; Malik, N.; Poppe, E.; Moe, S.T.; Finstad, T.G. Al-Al wafer-level thermocompression bonding applied for MEMS. In *Proceedings of the 2017 5th International Workshop on Low Temperature Bonding for 3D Integration (LTB-3D), Tokyo, Japan, 16–18 May 2017*; IEEE: Piscataway, NJ, USA, 2017; p. 11.
45. Zhu, Z.; Xia, K.; Fu, J.; Du, C.; Zhang, H.; Lou, H.; Xu, Z. Bonding of aluminum coated silicon wafers based on polypropylene carbonate and as a multi-functional sensor. *Org. Electron.* **2018**, *63*, 296–299. [CrossRef]
46. Lin, H.; Stevenson JT, M.; Gundlach, A.M.; Dunare, C.C.; Walton, A.J. Direct Al–Al contact using low temperature wafer bonding for integrating MEMS and CMOS devices. *Microelectron. Eng.* **2008**, *85*, 1059–1061. [CrossRef]
47. Chang, J.; Lin, L. MEMS packaging technologies & applications. In Proceedings of the 2010 International Symposium on VLSI Design, Automation and Test, Hsinchu, Taiwan, 26–29 April 2010; IEEE: Piscataway, NJ, USA, 2010; pp. 126–129.
48. Zhu, Z.; Yu, M.; Jin, Y. Investigations of silicon wafer bonding utilizing sputtered Al and Sn films. *Microsyst. Technol.* **2017**, *23*, 929–933. [CrossRef]
49. Satoh, S.; Fukushi, H.; Esashi, M.; Tanaka, S. Role of Thin Sn Layer for Low Temperature Al-Al Thermo-compression Bonding of Wafer-Level Hermetic Sealing. *Electron. Commun. Jpn.* **2018**, *101*, 33–40. [CrossRef]
50. Zhu, Z.; Yu, M.; Tian, D.; Zhu, Y.; Wang, P.; Liu, C.; Wang, W.; Miao, M.; Chen, J.; Jin, Y. Aluminum-coated silicon wafer bonding with tin intermediate layer. *J. Micro/Nanolithography MEMS MOEMS* **2013**, *12*, 013012. [CrossRef]

Disclaimer/Publisher's Note: The statements, opinions and data contained in all publications are solely those of the individual author(s) and contributor(s) and not of MDPI and/or the editor(s). MDPI and/or the editor(s) disclaim responsibility for any injury to people or property resulting from any ideas, methods, instructions or products referred to in the content.